

## The influence of glucose concentration upon the transport of light in tissue-simulating phantoms

Matthias Kohl†, Matthias Essenpreis‡ and Mark Cope†

† Department of Medical Physics and Bioengineering, University College London, 1st Floor Shropshire House, 11–20 Capper Street, London WC1E 6JA, UK

‡ Boehringer Mannheim, Sandhofer Strasse 116, 68305 Mannheim, Germany

Received 23 December 1994

**Abstract.** The effect of glucose upon the transport of light in tissue-simulating phantoms is shown and its possible application for non-invasive glucose monitoring in diabetic patients is discussed. The aim of this paper is to investigate the physical background of this effect.

The presence of glucose in an aqueous solution increases its refractive index and therefore has an influence upon the scattering properties of particles suspended in solution. Experimental data on the effect of glucose upon the scattering coefficient and the phase function of aqueous suspensions of spherical polystyrene particles are presented for near-infrared wavelengths and compared to values predicted by Mie theory. The subsequent effect upon light transport in multiple scattering, tissue-simulating phantoms is demonstrated experimentally in a slab geometry and theoretically by applying diffusion theory. It is furthermore shown that optional measurements in the frequency domain allow changes of absorption and scattering coefficient to be separately determined. The possible magnitude of this glucose effect in tissue *in vivo* is discussed.

### 1. Introduction

A continuous non-invasive method for monitoring body glucose concentrations would be of great advantage for diabetic patients. At present, these patients, who need to measure their glucose levels many times a day, rely on pricking their fingers to obtain blood samples. A drop of blood is placed upon a test strip, which undergoes a colour change due to an enzymatic chemical reaction. Nevertheless, it has been shown that the longer-term secondary effects of diabetes, such as retinopathy, nephropathy, neuropathy and microangiopathy/macroangiopathy can be significantly reduced by controlling the extent of blood glucose swings through more frequent monitoring (DCCT 1993).

Many techniques have been suggested for the monitoring of glucose, ranging from implanted electrochemical sensors (Wilson *et al* 1992) to non-invasive optical methods. The proposed optical methods are based upon photoacoustic (Quan *et al* 1993), absorbance or Fourier transform spectroscopy in the infrared region (Robinson *et al* 1992, Arnold and Small 1990, Kajiwara *et al* 1993, Marbach *et al* 1993). So far, none of these methods has proven to be sensitive or accurate enough for *in vivo* monitoring.

Here we follow a recently proposed method (Simonsen and Bucker 1994) that is based upon changes of the refractive index induced by glucose dissolved in aqueous solution. First investigations of this effect in tissue-simulating phantoms (Kohl *et al* 1994) and studies with volunteers (Maier *et al* 1994) have been published concurrently. The aim of this paper is

**Table 1.** A summary of the effect of glucose upon the basic optical properties of a phantom and the light transport within this phantom.

Effect of added glucose on basic optical properties of phantom		
Change in absorption properties		
(a) $\Rightarrow$ water absorption coefficient	$\mu_a^w \downarrow$	displacement of water (0.011% mM <sup>-1</sup> )
(b) $\Rightarrow$ intrinsic glucose absorption coefficient	$\mu_a^g \uparrow$	experiment: $\mu_a^w, \mu_a^g$ (figure 2)
Change in scattering properties		
(c) refractive index of suspending medium	$\Delta_g n \uparrow$	$\Delta_g n = 2.5 \times 10^{-5}$ mM <sup>-1</sup>
(d) $\Rightarrow$ scattering coefficient	$\mu_s \downarrow$	polystyrene ( $d = 1.27 \mu\text{m}$ , 800 nm) in water
(e) $\Rightarrow$ phase function $p \Rightarrow$	$g$ value $\uparrow$	$\delta_g \mu_s = -0.015\%$ , $\Delta_g g = 8.5 \times 10^{-6}$ mM <sup>-1</sup>
(f) $\Rightarrow$ modified scattering coefficient	$\mu'_s = \mu_s(1 - g) \downarrow$	$\delta_g \mu'_s = -0.023\%$ mM <sup>-1</sup> (figures 3–5)
Effect of added glucose on light transport in tissue-simulating phantoms		
(g) $\Rightarrow$ transmittance	$T \uparrow$	experiment: cuvette (figures 7–9)
(h) $\Rightarrow$ phase shift	$\Phi \uparrow$	diffusion theory for slab geometry: using (a)–(f) mismatched boundary condition

to describe the influence of glucose upon light transport in tissue-simulating phantoms and to expand upon the results of a previously published letter (Kohl *et al* 1994).

When glucose is added to an aqueous suspension of inert scattering particles a number of physical effects that are summarized in table 1 may change the propagation of light in the scattering medium. Glucose reduces the absorption coefficient  $\mu_a^w$  of the water in the aqueous solution because it displaces water (i.e. reduces the molar concentration of water molecules). At the same time it adds the intrinsic glucose absorption coefficient  $\mu_a^g$  (table 1(a), (b)). The refractive index  $n$  of the aqueous solution increases with the glucose concentration (table 1(c)), resulting in a reduced velocity of light and a changes of the scattering properties of particles (scattering coefficient  $\mu_s$ , phase function  $p$  and  $g$  value) suspended in the solution (table 1(d)–(f)). To investigate and separate these effects, experimental results were compared with predictions from Mie theory. Finally, the subsequent effect of these changes in refractive index, the absorption and the scattering coefficient upon the transport of light in multiple scattering, tissue-simulating phantoms was investigated (table 1(g), (h)). Measurements are made of the changes of the transmittance and phase delay of intensity modulated light in a slab geometry. These results can be described by diffusion theory. Additionally, a method to separate the changes in the absorption and scattering coefficient is introduced.

The implications of these phantom studies for the potential non-invasive detection of glucose in tissue are discussed in the final section of this paper.

## 2. The effect of glucose on the optical properties of a phantom

### 2.1. Method and experimental set-up

The attenuation of light transmitted through a suspension of particles is due to absorption and scattering (characterized by the absorption coefficient  $\mu_a(\lambda)$  and the scattering coefficient  $\mu_s(\lambda)$  respectively) and can be described by the total attenuation coefficient  $\mu_t(\lambda)$  that is

given by

$$\mu_t(\lambda) = \mu_s(\lambda) + \mu_a(\lambda) = (1/z) \ln[I_0(\lambda)/I(\lambda)] \quad (1)$$

where  $z$  is the physical pathlength of the suspension and  $I_0(\lambda)$  and  $I(\lambda)$  are the transmitted light intensities at the wavelength  $\lambda$  through the cuvette containing the reference solution (normally pure water) and the suspension under investigation, respectively. Either  $\mu_s(\lambda)$  or  $\mu_a(\lambda)$  can then be calculated from  $\mu_t(\lambda)$  as long as changes of the other coefficient can be neglected or be subtracted. Equation (1) is valid for the single scattering regime, i.e. as long as the probability of scattered light being detected is negligible.

Experimentally, the absorption and scattering coefficients of a solution were determined with a collimated beam set-up. This set-up measured the transmitted intensities of a cuvette containing the solution under investigation and consisted of a quartz lamp (100 W) serving as a light source and a spectrophotometer. The light was delivered by an optical fibre (100  $\mu\text{m}$  core diameter) and collimated by a lens (focal length, 16 mm) producing a beam diameter of approximately 2 mm. To collect the transmitted light an identical lens/fibre combination was positioned collinearly. Because the acceptance angle of this light collecting lens (distance about 50 cm) was small (half angle  $\alpha = 3 \times 10^{-3}$  rad) and the scattering particle density was low, the probability of scattered light being detected was negligible. The spectrophotometer consisted of a grating monochromator in combination with a nitrogen-cooled charge-coupled device (CCD) (Cope 1991). The sensitivity of the detector limited the spectra to wavelengths  $\lambda < 1030$  nm with data at wavelengths greater than 950 nm being of limited use because of low sensitivity. This set-up was used in either a horizontal or vertical arrangement as described later.

## 2.2. Scattering by spherical particles

Mie theory was used to calculate the scattering coefficient, the phase function and the  $g$  value of spherical particles of arbitrary diameter  $d$  in an analytical form from the refractive indices of both the spheres  $n_s$  and the medium  $n_m$  and the wavelength  $\lambda$  of the light. Here an algorithm given by Bohren and Huffman (1983) was applied to spherical polystyrene particles suspended in water. To include the wavelength dependence of the refractive indices, data given by Weast (1974) and Kaye and Laby (1986) for the refractive index of water  $n_w$  and polystyrene  $n_p$  for visible wavelengths were extrapolated into the near-infrared region. To that end the dispersion function of the refractive indices was approximated by a Cauchy fit (Hecht 1987) of the form  $n(\lambda) = n_0 + n_2/\lambda^2 + n_4/\lambda^4 + n_6/\lambda^6$ . The following fit parameters (for  $\lambda$  in nanometres) were found for water and polystyrene:

$$\text{water:} \quad n_0 = 1.3199 \quad n_2 = 6.878 \times 10^3 \quad n_4 = -1.132 \times 10^9 \\ n_6 = 1.11 \times 10^{14}$$

$$\text{polystyrene:} \quad n_0 = 1.5626 \quad n_2 = 1.169 \times 10^4 \quad n_4 = -1.125 \times 10^9 \\ n_6 = 1.72 \times 10^{14}.$$

Two batches of polystyrene particles of different size distributions were used. For a batch of spherical particles with a narrow size distribution ( $d = 1.27(\pm 0.09)$   $\mu\text{m}$ , Seradyn, Indianapolis, IN) it was sufficient to perform the Mie calculations with the mean diameter. The second batch of particles (B Harness, Department of Chemical Engineering, University of Bradford) had a broad distribution of diameters in the range  $4 \mu\text{m} < d < 7 \mu\text{m}$

(measured in a Coulter counter). This was accounted for by dividing the distribution into 20 subranges whose mean diameters were equally separated by  $0.15 \mu\text{m}$ . Mie calculations were performed for each subrange and the results averaged after weighting according to the relative fraction of particles falling within each subrange. It was assumed that absorption of light by polystyrene was negligible.

### 2.3. The effect of glucose on the refractive index

The increase  $\Delta_g n(c_g)$  of the refractive index  $n$  of an aqueous solution of glucose with increasing glucose concentration  $c_g$  is given by Weast (1974) for visible wavelengths,

$$\Delta_g n = 2.5 \times 10^{-5} / \text{mM glucose} \quad (2)$$

and was assumed to be identical over the whole wavelength region under investigation.

### 2.4. The effect of glucose on the absorption coefficient

The absorption coefficients of water and aqueous glucose solutions had to be accurately determined in order to model the light transport in the multiple-scattering phantom. The effect of glucose upon the absorption coefficient is twofold. Firstly, glucose reduces the molarity  $C_w(c_g)$  of water and accordingly the contribution of water to the absorption coefficient of the aqueous glucose solution is  $[C_w(c_g)/C_w^0]\mu_a^w$ , where  $\mu_a^w$  is the absorption coefficient of pure water of molarity  $C_w^0$ . For a temperature  $T = 20^\circ\text{C}$  the molarity of water for zero glucose concentration is  $C_w^0 = C_w(c_g = 0 \text{ mM}) = 55.4 \text{ M}$  and decreases with increasing glucose concentration to  $C_w(c_g = 200 \text{ mM}) = 54.17 \text{ M}$  (Weast 1974). Secondly, the overall absorption increases due to the 'intrinsic' glucose absorption  $\mu_a^g(c_g)$ . Table 2 summarizes how  $\mu_a^w$ ,  $\mu_a^g(c_g)$  and the difference in absorption between a glucose solution and pure water ( $\mu_a^{wg}(c_g)$ ) were derived from measurements of transmitted light intensities. In our experiments, the collimated beam set-up either aligned horizontally (figure 1(a)) or aligned vertically (figure 1(b)) was used. In the vertical alignment the collimated beam traverses the rectangular cuvette perpendicularly from underneath and allows the pathlength  $z$  to change with increases in the volume of the solution. The drawback of this alignment is that the surface of a solution is never perfectly plane and slight lateral deflections of the beam occur. Therefore a detector with a larger acceptance angle was used for absorption coefficient measurements. An integrating sphere (diameter 7 cm) was used with an aperture diameter of 1 cm and connected to a spectrophotometer via a fibre bundle. The acceptance angle was approximately  $\alpha = 2.5 \times 10^{-2}$  rad. Since in this case the solution did not contain any scattering particles, the larger acceptance angle did not affect  $\mu_a$  determination.

Table 2. Experimental conditions for the measurement of the absorption coefficient of water and glucose-induced absorption changes.

Absorption coefficient	Experimental conditions
(I) water absorption $\mu_a^w = 1/(z_2 - z_1) \ln[I(z_1)/I(z_2)]$	Vertical, different volumes $\Rightarrow (z_1, z_2)$
(II) intrinsic glucose absorption $\mu_a^g(c_g) = 1/z_g \ln[I(c_g = 0, z_0)/I(c_g, z_g)]$	Vertical, water ( $z_0$ ), glucose added ( $z_g$ )
(III) intrinsic glucose absorption $= 1/z \ln[I(c_g = 0, z)/I(c_g, z)]$ minus water absorption $\mu_a^{wg}(c_g) = \mu_a^g(c_g) - \mu_a^w(1 - C_w(c_g)/C_w^0)$	Horizontal, same pathlength $z$  Calculated, from (I) and (II) with molarity of water $C_w(c_g), C_w^0$

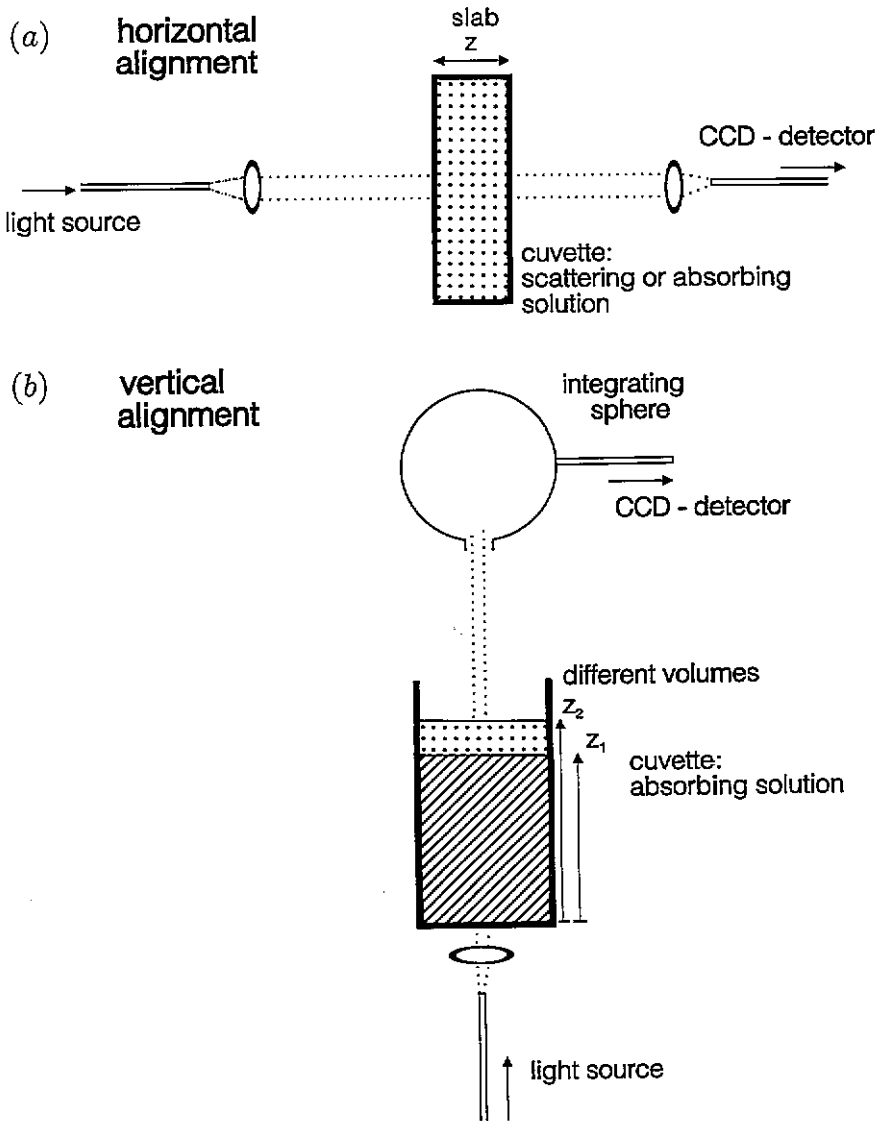


Figure 1. The collimated beam set-up for measuring the total attenuation coefficient  $\mu_t = \mu_a + \mu_s$ : (a) horizontal alignment; (b) vertical alignment.

The absorption of pure water was derived by measuring the transmitted light intensities  $I_1(z_1)$  and  $I_2(z_2)$  through different pathlengths  $z_1 = 5$  mm and  $z_2 = 70$  mm of pure water using the vertical set-up:

$$\mu_a^w = 1/(z_2 - z_1) \ln[I_1(z_1)/I_2(z_2)]$$

(table 2(I)). The intrinsic absorption of the glucose solution  $\mu_a^g(c_g)$  was measured in the vertical set-up by dissolving known weights of glucose in pure water. The advantage of the vertically aligned set-up is that it enables  $\mu_a^g(c_g)$  to be measured directly without any need for corrections. While glucose reduces the molarity of water in an aqueous solution, the volume (i.e. the pathlength) is increased. Hence the total number of water molecules

crossed by the light and contributing to the absorption is not affected by the changing glucose concentration.  $\mu_a^g(c_g)$  can be directly calculated from the transmitted intensities  $I_0$  ( $c_g = 0$  mM) (pathlength  $z_0$ ) and  $I_g(c_g)$  (pathlength  $z_g$ ) of a constant volume of water before and after glucose was added:  $\mu_a^g(c_g) = 1/z_g \ln[I_0/I_g]$  (table 2(II)).

The vertical arrangement of light source/detector is somewhat unusual. Normally absorption measurements are made in a horizontal arrangement comparing the transmitted intensities of pure water and glucose solution at the same pathlength  $z$  (table 2(III)). The logarithmic ratio of intensities under these conditions,  $\mu_a^{wg}(c_g)$ , is the difference of the intrinsic absorption coefficient of glucose in an aqueous solution and the absorption coefficient that corresponds to the displaced water. The intrinsic glucose absorption can then be calculated according to  $\mu_a^g(c_g) = \mu_a^{wg}(c_g) + \mu_a^w(1 - C_w(c_g)/C_w^0)$ , where the ratio of the molarity of water in an aqueous glucose solution  $C_w(c_g)$  and pure water  $C_w^0$  has been included. Using values for the displacement of water by glucose  $D(c_g) = (1 - C_w(c_g)/C_w^0) = -0.0111\% \text{ mM}^{-1}$  given by Weast (1974),  $\mu_a^{wg}(c_g)$  was calculated. For a concentration of  $c_g = 200$  mM, the calculated spectrum of  $\mu_a^{wg}(c_g)$  was found to be in agreement with the directly measured spectrum.

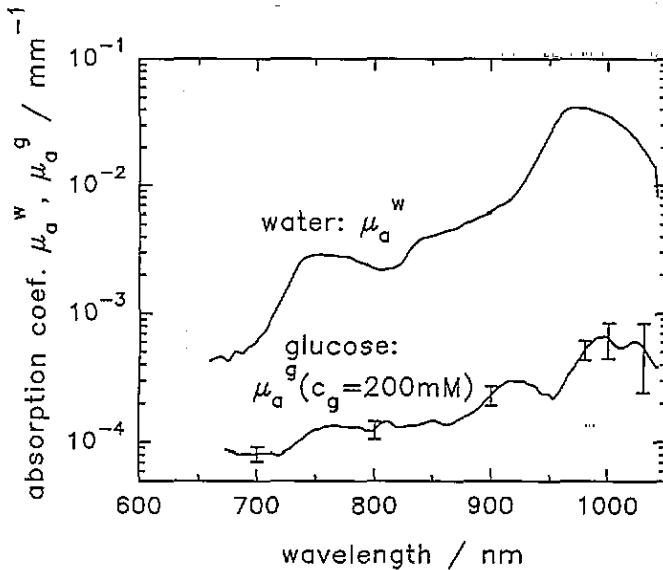


Figure 2. The absorption coefficient of water  $\mu_a^w$  and intrinsic glucose absorption in water  $\mu_a^g$  ( $c_g = 200$  mM) at  $T = 21^\circ\text{C}$ .

In figure 2 the measured spectra of the absorption coefficient of pure water  $\mu_a^w(\lambda)$  and the intrinsic glucose absorption  $\mu_a^g(\lambda, c_g)$  for  $c_g = 200$  mM are shown. As the change of  $\mu_a^w(\lambda)$  with temperature is considerable (about  $+0.5\% \text{ }^\circ\text{C}^{-1}$  at 960 nm) the temperature was carefully kept constant at  $21^\circ\text{C}$ . The water absorption spectrum is in agreement with values given by Hale and Querry (1973) and Kou *et al* (1993).

### 2.5. The effect of glucose on the scattering coefficient

All scattering coefficients were derived from measurements in the horizontally aligned collimated beam set-up with the low-acceptance-angle detector ( $\alpha = 3 \times 10^{-3}$  rad) described initially.

The wavelength dependence of the scattering coefficient  $\mu_s(\lambda)$  of a suspension of polystyrene microspheres of diameter  $d = 1.27(\pm 0.09) \mu\text{m}$  and concentration  $c_s = 0.0019\%$  v/v was determined from transmission spectra through a cuvette of pathlength  $z = 20 \text{ mm}$  according to equation (1). The glucose concentration  $c_g$  was varied in eight steps between 0 and 144 mM.

Adding pure glucose results in an increase of the suspension's volume, i.e. in a change of the water concentration (molarity) and sphere concentration  $c_s$ . Here a dilution of the sphere concentration was averted by adding glucose within an aqueous suspension of the same concentration  $c_s$ . A change of water molarity could not be avoided. Nevertheless,  $\mu_s$  was obtained from the measured total attenuation coefficient  $\mu_t$  by correcting for changes of the absorption coefficient using  $\mu_a^{wg}$ . In figure 3 the resulting spectra  $\mu_s(\lambda)$  are shown for  $c_g = 0 \text{ mM}$  and 144 mM. For the whole range of wavelengths under investigation  $\mu_s$  decreases monotonically with wavelength and is lower for  $c_g = 144 \text{ mM}$ . Predictions from Mie theory calculated for refractive indices of the medium corresponding to  $c_g = 0 \text{ mM}$  and  $c_g = 144 \text{ mM}$  are also shown. The agreement between theoretical and experimental  $\mu_s$  is good. Deviations might be due to errors in the absolute values of the refractive index obtained by extrapolation of visible wavelength data.

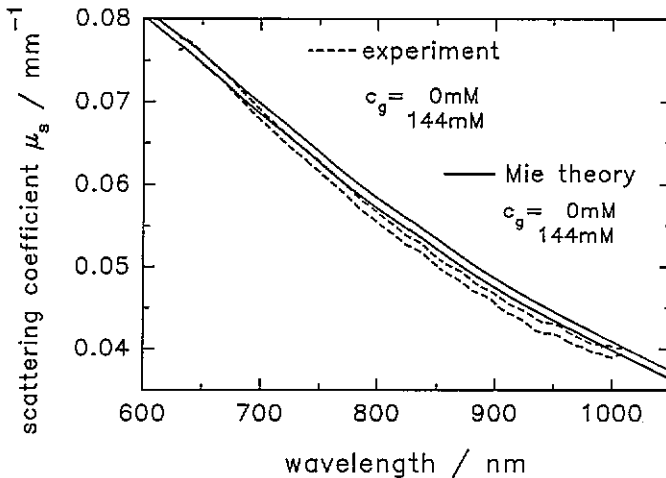


**Figure 3.** The measured total attenuation coefficient  $\mu_t$  of polystyrene spherical particles ( $d = 1.27(\pm 0.09) \mu\text{m}$ ,  $c_s = 0.0019\%$  v/v) for aqueous glucose concentrations of  $c_g = 0 \text{ mM}$  and 144 mM (upper and lower dashed line, respectively). The scattering coefficient  $\mu_s$  calculated from Mie theory for the corresponding refractive indices of the aqueous solutions is also shown (solid lines).

To investigate the change of the scattering coefficient with glucose concentration in detail, the fractional change  $\delta_g \mu_s(c_g) = 2[\mu_s(c_g) - \mu_s(c_g = 0 \text{ mM})] / [\mu_s(c_g) + \mu_s(c_g = 0 \text{ mM})]$  of the scattering coefficient was calculated and is shown in figure 4 for  $c_g = 85 \text{ mM}$  and 144 mM. For  $\lambda < 920 \text{ nm}$  the agreement between experimental and predicted  $\delta_g \mu_s$  is excellent whereas for longer wavelengths the interpretation of the spectra is aggravated by high noise caused by a low signal intensity. This is due to the low sensitivity of the CCD detector as well as the high absorption of water and the small scattering coefficient in this part of the spectrum. For the range of glucose concentration studied

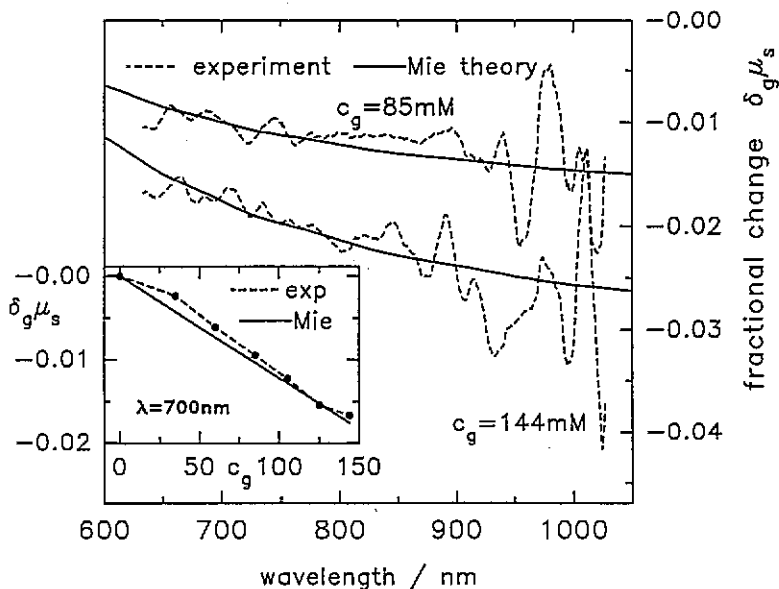
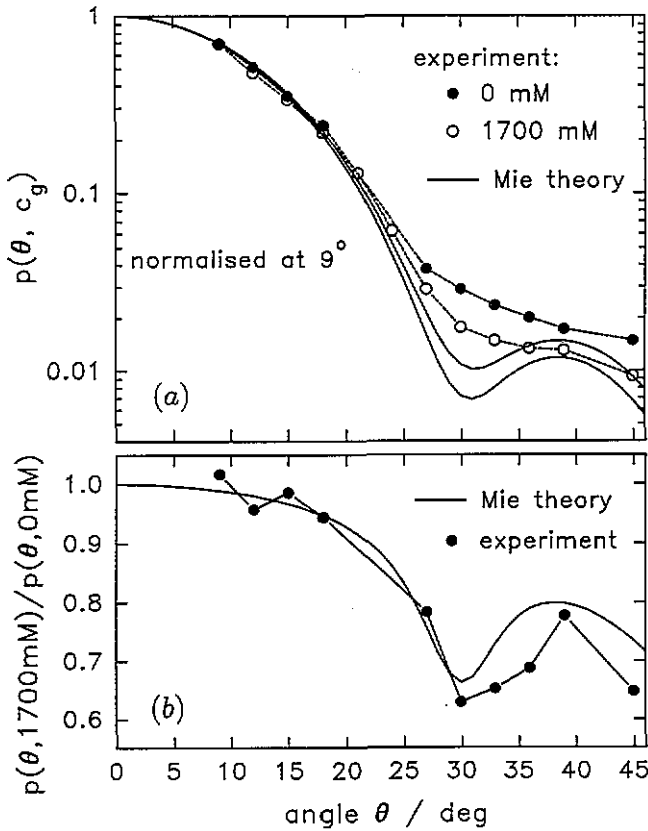


Figure 4. The fractional change  $\delta_g \mu_s(c_g) = 2[\mu_s(c_g) - \mu_s(c_g = 0 \text{ mM})]/[\mu_s(c_g) + \mu_s(c_g = 0 \text{ mM})]$  in the scattering coefficient for glucose concentrations of  $c_g = 85 \text{ mM}$  and  $144 \text{ mM}$ . The experimental data (dashed lines) are compared with predictions from Mie theory (solid lines). The inset shows the dependence of  $\delta_g \mu_s$  on  $c_g$  for  $\lambda = 700 \text{ nm}$ .

here ( $0 \text{ mM} < c_g < 144 \text{ mM}$ )  $\delta_g \mu_s$  decreases linearly with concentration and has values of about  $\delta_g \mu_s = -0.012\% \text{ mM}^{-1}$  at  $\lambda = 700 \text{ nm}$  and  $-0.016\% \text{ mM}^{-1}$  at  $\lambda = 955 \text{ nm}$  (see the inset of figure 4).

## 2.6. The effect of glucose on the phase function and $g$ value

The experimental set-up that allowed measurement of the phase function  $p(\theta)$ , i.e. the dependence of the scattered light intensity on the scattering angle  $\theta$ , has been described in detail by Firbank *et al* (1993). It includes the same light source and detector system as used in the collimated beam experiments in combination with a goniometer turntable. The liquid sample could be sandwiched between two glass hemicylinders (65 mm diameter) with an antireflection coating. In figure 5(a) the measured phase function  $p(\theta)$  of the same batch of polystyrene spheres ( $d = 1.27 \text{ nm}$ ) as studied in the experiments described above is shown for angles  $0^\circ \leq \theta \leq 45^\circ$  and compared with calculations from Mie theory. Unpolarized light at  $\lambda = 700 \text{ nm}$  was used. As the predicted change with changing refractive index of the medium is small, the phase function was measured for  $c_g = 0 \text{ mM}$  and  $c_g = 1700 \text{ mM}$  corresponding to  $\Delta_g n = 0.0425$ . The calculated intensities at  $\theta = 9^\circ$  were used to normalize the experimental phase functions. There is a coarse agreement between calculated and experimental phase functions although the local minimum of the scattered intensity near  $\theta = 30^\circ$  was not observed in the experimental data. This might be partly due to deficiencies in the experimental set-up (polarization effects, insufficient angular resolution), an imperfect spherical shape and a possible aggregation of the particles. Nevertheless, there is a considerable agreement between the theoretical and the measured ratio of the phase functions  $p(\theta, 1700 \text{ mM})/p(\theta, 0 \text{ mM})$  shown in figure 5(b). This ratio has a distinct



**Figure 5.** (a) The phase function  $p(\theta, c_g)$  of polystyrene spheres ( $d = 1.27(\pm 0.09)$   $\mu\text{m}$ ) for unpolarized light of  $\lambda = 700$  nm. The experimental data are shown for zero glucose concentration (filled circles) and  $c_g = 1700$  mM (hollow circles). Predictions from Mie theory are shown (solid lines) and have been used for normalization of the experimental intensities at  $\theta = 9^\circ$ . (b) The ratio of the phase functions  $p(\theta, c_g = 1700 \text{ mM})/p(\theta, c_g = 0 \text{ mM})$ . The four experimental values for  $9^\circ \leq \theta \leq 18^\circ$  were used for normalization.

minimum near  $\theta = 30^\circ$  and is less than unity for  $\theta > 20^\circ$ , indicating that for the higher glucose concentration the scattered light is more forward peaked. Hence the  $g$  value, i.e. the mean cosine of the phase function ( $g = \int [p(\theta) \cos(\theta) \sin(\theta) d\theta] / \int [(p(\theta) \sin(\theta) d\theta)]$ ), is higher for higher glucose concentrations: Mie theory predicts  $g(c_g = 0 \text{ mM}) = 0.9283$  and an absolute change  $\Delta_g g = 8.45 \times 10^{-6} \text{ mM}^{-1}$  glucose at 700 nm.

**2.7. The effect of glucose on the modified scattering coefficient**

For multiple-scattering media, the reduced scattering coefficient  $\mu'_s = \mu_s(1-g)$  characterizes the light transport when it is modelled by diffusion theory and its fractional sensitivity to glucose is  $\delta_g \mu'_s = \delta_g \mu_s - \Delta_g g / (1-g)$ . Inserting the values given above for polystyrene particles of  $d = 1.27 \mu\text{m}$  shows that  $\Delta_g g$  and  $\delta_g \mu_s$  contribute approximately equally to  $\delta_g \mu'_s$  for the particle diameter and wavelength studied:  $\delta_g \mu'_s = -0.023\% \text{ mM}^{-1}$  at 700 nm.

In the multiple-scattering experiments the second batch of polystyrene particles with the broad size distribution of  $4 \mu\text{m} < d < 7 \mu\text{m}$  was used. The calculated spectrum  $\mu_s(\lambda)$  of these particles had a distinct 'ripple' structure with variations of up to  $\pm 3\%$  and a separation

of the maxima of about 25 nm. This 'ripple' structure is probably caused by artefacts in the Mie calculation due to the limited number of subranges used for the size distribution of the polystyrene spheres. The ripples were not found experimentally. After smoothing out these ripples the calculated and experimental spectra were in good agreement. The calculated  $g$  value was between 0.85 and 0.88, giving a  $\mu'_s$  relatively independent of wavelength with values between  $\mu'_s = 0.880 \text{ mm}^{-1}$  ( $\lambda = 700 \text{ nm}$ ) and  $\mu'_s = 0.898 \text{ mm}^{-1}$  ( $\lambda = 1000 \text{ nm}$ ) for a concentration of 1% v/v. The magnitude of the relative change  $\delta_g \mu'_s$  was larger for higher wavelengths and had values of  $\delta_g \mu'_s = -0.011\%$  for  $\lambda = 700 \text{ nm}$  and  $-0.020\%$  for  $\lambda = 1000 \text{ nm}$  per mM glucose concentration. These calculated values of the modified scattering coefficient  $\mu'_s$  were used in the following experiments.

### 3. The effect of glucose upon the light transport in multiple-scattering phantoms

Following the investigation of the influence of glucose concentration upon the single-scattering properties of spherical particles, experiments were performed to assess the transport of light and its dependence on glucose concentration in multiple-scattering, tissue-simulating phantoms.

Here the results of two experiments are presented, both performed in a slab geometry. The aim of the first experiment is to describe changes of the transmitted light intensity, i.e. the transmittance, and emphasizes the relevance of the magnitude of absorption to the overall glucose effect. In the second experiment, the glucose-induced change of transmittance and phase shift of an intensity-modulated light source was examined. A simple method to separate changes of the absorption and scattering coefficient is explained and tested on the experimental data. All the experimental results were validated with diffusion theory predictions.

#### 3.1. Diffusion theory for slab geometry

During the last few years diffusion theory has been expanded to describe the temporal characteristics of the transport of light in homogeneous media of simple geometry. For an incident 'pencil' light beam the intensity of the reflected and transmitted light as well as its temporal spreading or the phase of an intensity-modulated light source can be calculated from  $\mu'_s$ ,  $\mu_a$  and the refractive index  $n_m$  of the medium (Patterson *et al* 1989, Arridge *et al* 1992). This theory is the appropriate tool to describe the experimental results obtained on the transmission side of a slab.

The infinite slab of thickness  $L$  outlined in figure 6 is characterized by  $\mu'_s$ ,  $\mu_a$  and the refractive index  $n_m$ . Here we are interested in the transmittance  $T(z = L, r)$  at the position  $(z = L, r)$  as well as the phase  $\Phi(z = L, r)$  of the transmitted light of an light source modulated at a frequency  $\nu_M$ . For  $T(z = L, r)$  and the mean transit time  $\langle t \rangle(L, r)$  there are analytical solutions for slab geometry (Patterson *et al* 1989, Arridge *et al* 1992). Unfortunately, the phase  $\Phi(L, r)$  cannot be expressed in simple form for this geometry (Arridge *et al* 1992). Therefore the approximate linear relationship between phase and mean time,  $\Phi = -2\pi\nu_M\langle t \rangle$  (Duncan *et al* 1993) where  $\nu_M$  is the modulation frequency, was used to calculate  $\Phi$  from  $\langle t \rangle$ .

Patterson *et al* (1989) and Arridge *et al* (1992) give both  $T$  and  $\langle t \rangle$  in terms of an infinite series of dipole terms, each of which ensures that the photon fluence rate is zero at the boundaries at  $z = 0$  and  $z = L$  of the infinite slab. In the experimental conditions the photon fluence rate is greater than zero at the boundaries because of specular reflections due to different refractive indices of the solution, the cuvette and air. The resulting mismatched

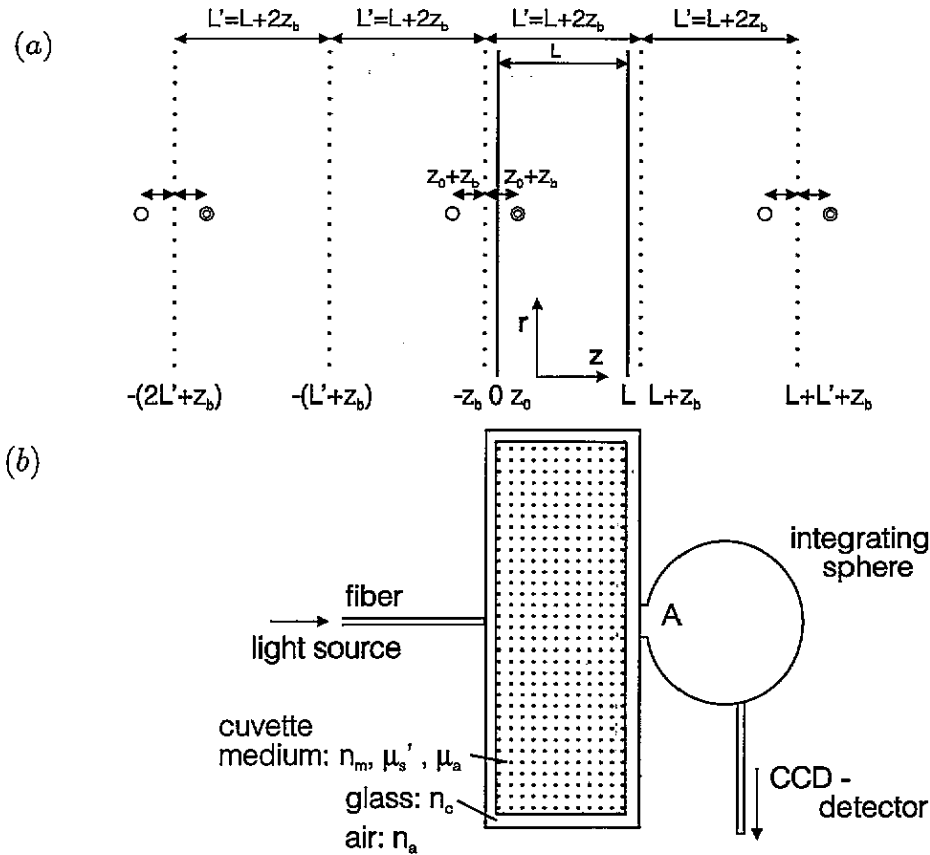


Figure 6. An illustration of the slab geometry: (a) the positions of the first three dipole terms used in diffusion theory; (b) the experimental conditions.

boundary conditions can be taken into account by the method of extrapolated boundaries (Keijzer *et al* 1988, Farrell and Patterson 1992, Moulton 1990): The position of each dipole is chosen to make the fluence rate zero on the surfaces  $z = -z_b$  and  $z = L + z_b$  where  $z_b$  is a constant depending on the specular reflection. The transmittance  $T$  and the mean transit time  $\langle t \rangle$  can then be written as infinite sums:

$$T(L, r) = \sum_{i=0}^{\infty} [F(L + 2iL' - z_0) - F(L + 2iL' + z_0 + 2z_b) + F(L + 2iL' - z_0 + 2z_b) - F(L + 2iL' + z_0 + 4z_b)] \tag{3}$$

with

$$F(x) = (1/4\pi)x \left\{ \left[ \exp(-\mu_{\text{eff}}\sqrt{x^2 + r^2}) \right] / (x^2 + r^2) \right\} (\mu_{\text{eff}} + 1/\sqrt{x^2 + r^2}) \tag{4}$$

and

$$\langle t \rangle(L, r) = \frac{1}{T(L, r)} \sum_{i=0}^{\infty} [H(L + 2iL' - z_0) - H(L + 2iL' + z_0 + 2z_b) + H(L + 2iL' - z_0 + 2z_b) - H(L + 2iL' + z_0 + 4z_b)] \tag{5}$$

with

$$H(x) = (\pi D/2c)x \left[ \exp\left(-\mu_{\text{eff}}\sqrt{x^2 + r^2}\right) \right] / (x^2 + r^2) \quad (6)$$

where the effective attenuation coefficient is  $\mu_{\text{eff}} = (3\mu_a(\mu_a + \mu'_s))^{1/2}$  and the diffusion constant  $D = (3(\mu_a + \mu'_s))^{-1}$ . Furthermore,  $z_0 = 1/\mu'_s$  and  $c = c_0/n_m$  is the light velocity in the medium (speed of light in vacuum,  $c_0$ ).  $L' = L + 2z_b$  is the effective pathlength of the cuvette with  $z_b = 2AD$  where the internal reflection parameter  $A$  can be approximated by (Keijzer et al 1988, Farrell and Patterson 1992)

$$A = [2/(1 - R_0) - 1 + |\cos \Theta_c|^3] / (1 - |\cos \Theta_c|^2). \quad (7)$$

Here both the critical refractive angle  $\Theta_c = \sin^{-1}(1/n_r)$  and  $R_0 = [(n_r - 1)/(n_r + 1)]^2$  depend on the relative refractive index  $n_r = n_m/n_a$  between the refractive index of the slab medium  $n_m$  and the surrounding  $n_a$ .

### 3.2. The influence of glucose upon transmitted light intensity

**3.2.1. Method.** The transmission spectra of a cuvette (size 60 mm  $\times$  80 mm, pathlength  $L = 20$  mm) containing an aqueous suspension of polystyrene particles were measured with a similar set-up as described previously (see figure 6(b)). A fibre bundle of 2.5 mm diameter positioned at one side of the cuvette delivered light from the halogen lamp while an integrating sphere (70 mm diameter, aperture area  $A = 25\pi$  mm<sup>2</sup>) placed at the opposite side of the cuvette was used to detect the spectrum  $I(\lambda)$  of the transmitted light. The known aperture of the integrating sphere allowed the spectrum to be normalized to the incident intensity and detector area  $A$ . A spectrum of the incident light  $I_N(\lambda)$  was recorded by placing the light delivering fibre bundle directly at the aperture of the integrating sphere. The transmitted intensity  $I(\lambda)$  was recorded with the cuvette placed against the integrating sphere. A partial specular reflection  $R$  (about 4%) of the incident light at the first air/cuvette boundary and the entry to the integrating sphere aperture  $A$  was taken into account to produce a normalized spectrum of the transmittance  $T(\lambda) = I(\lambda)/I_N(\lambda)(1 - R)A^{-1}$ , i.e.  $T(\lambda)$  is expressed in units of detector area. The optical properties of the phantom, which consisted of an aqueous suspension of polystyrene microspheres ( $4 \mu\text{m} < d < 7 \mu\text{m}$ ) at a concentration of  $c_s = 0.968\%$  v/v were  $\mu'_s = 0.852 \text{ mm}^{-1}$  ( $\delta_g \mu'_s = -0.011\% \text{ mM}^{-1}$ ) at  $\lambda = 700 \text{ nm}$  and  $\mu'_s = 0.870 \text{ mm}^{-1}$  ( $\delta_g \mu'_s = -0.020\% \text{ mM}^{-1}$ ) at  $\lambda = 1000 \text{ nm}$ . The absorption coefficients for pure water and the aqueous glucose solution were taken from figure 2.

At the boundaries of the experimental slab, specular reflections occurred due to the different refractive indices of the solution ( $n_m$  given above), the glass cuvette (thickness 2.5 mm,  $1.525 > n_c > 1.50$ ) and air ( $n_a = 1$ ). To include the mismatched boundary conditions in the calculation, a single parameter  $z_b$  describing the combined effect of these specular reflections had to be found. Therefore the specular reflection of the (dielectric) water-glass-air layer was calculated for diffuse, unpolarized radiation using equations based upon Maxwell's theory given by Kong (1986). It was found that the specular reflection can be approximately represented by a single boundary with a relative refractive index  $n_r = 1.367$  at  $\lambda = 700 \text{ nm}$  and  $n_r = 1.366$  at  $\lambda = 1000 \text{ nm}$ . The increment of the refractive index of the glucose solution  $\Delta_g n_m = 0.005$  for  $c_g = 200 \text{ mM}$  was taken into account by increasing  $n_r$  between 0.0015 (700 nm) and 0.0009 (1000 nm). These values for  $n_r$  were linearly interpolated between 700 nm and 1000 nm.

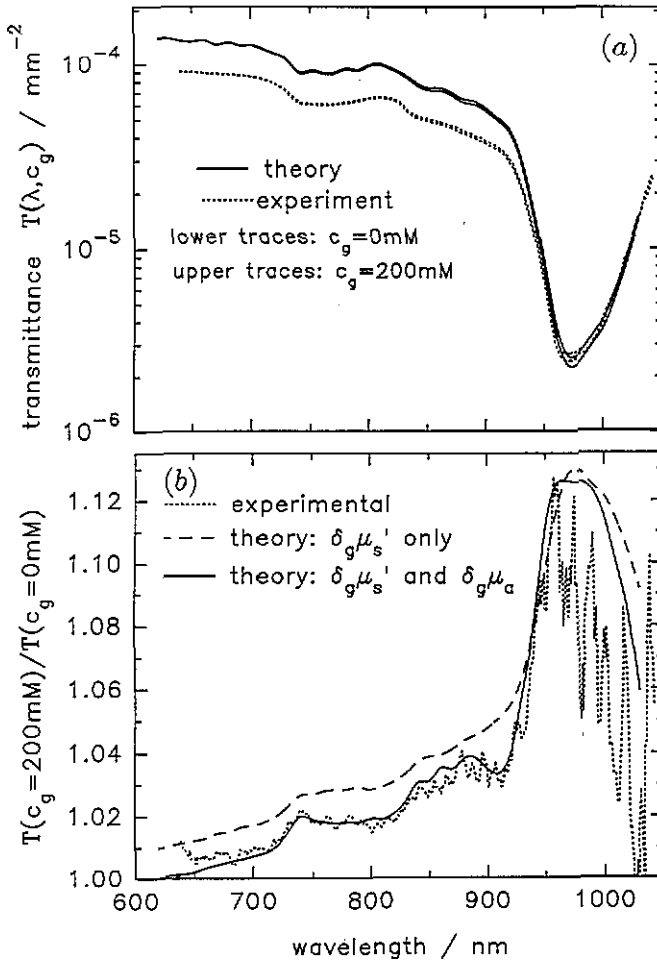


**Figure 7.** (a) Spectra of the normalized transmittance  $T(\lambda, c_g)$  in units of  $\text{mm}^{-2}$  of a cuvette (pathlength  $L = 20 \text{ mm}$ ) containing an aqueous suspension of polystyrene spherical particles ( $4 \mu\text{m} < d < 7 \mu\text{m}$ ,  $c_s = 0.968\% \text{ v/v}$ ) for glucose concentrations of  $c_g = 0 \text{ mM}$  (lower dotted line) and  $c_g = 200 \text{ mM}$  (upper dotted line). Predictions from diffusion theory for slab geometry are plotted for both glucose concentrations (lower and upper solid lines). No normalization was used. (b) The ratio  $T(\lambda, c_g = 200 \text{ mM}) / T(\lambda, c_g = 0 \text{ mM})$  of the transmittance spectra shown in (a). The experimental data (dotted line) can be compared with calculations from diffusion theory taking into account the glucose-induced changes of the scattering coefficient  $\delta_g \mu_s'$  (dashed line) and the change of both the scattering and the absorption coefficient (solid line).

**3.2.2. Results.** In figure 7(a) two experimental transmittance spectra  $T(\lambda, c_g)$  are shown for this phantom for zero glucose concentration (lower dotted line) and  $c_g = 200 \text{ mM}$  (upper dotted line). The ratio of the two spectra  $T(\lambda, c_g = 200 \text{ mM}) / T(\lambda, c_g = 0 \text{ mM})$  is plotted in figure 7(b) (dotted line). Using the values for the optical properties and the boundary conditions, the spectra  $T(\lambda, c_g)$  were calculated from (3) (solid lines in figure 7(a)). Within the absorption band of water near  $\lambda = 975 \text{ nm}$ , the calculated  $T$  (about  $2.5 \times 10^{-6} \text{ mm}^{-2}$ ) agrees with the experimental values whereas at the lower-wavelength end of the spectrum ( $T \approx 1 \times 10^{-4} \text{ mm}^{-2}$ ) the discrepancy is about 30%. The reason for the discrepancy at these lower wavelengths may be that absorption is small, i.e. the effective pathlength of

the photons in the medium is high. This might result in a stronger influence of the limited size of the cuvette and subsequently a difference from the theoretical value that is based upon an infinite slab. For wavelengths with a higher absorption this influence is smaller because the path of the photons is more likely to be confined to the centre of the cuvette. Nevertheless, the overall agreement between theory and experiment is good. As  $\mu'_s(\lambda)$  is fairly wavelength independent, the spectra reflect predominantly the absorption properties of water (compare with figure 2). For all wavelengths the transmitted intensity is higher for  $c_g = 200$  mM than for zero glucose concentration. These differences are small but can clearly be seen in the plot of the ratio  $T(\lambda, c_g = 200 \text{ mM})/T(\lambda, c_g = 0 \text{ mM})$  shown in figure 7(b). This ratio varies between less than 1.01 for 700 nm and more than 1.10 within the absorption band of water. To compare the experimental with the theoretical ratio and to illustrate the contribution of the magnitude of changes in absorption and scattering, firstly only the effect of glucose upon the scattering coefficient has been included (the dashed line of figure 7(b)), resulting in a ratio that is higher than that observed for the experimental data for all wavelengths less than 920 nm. By including changes of absorption coefficient (water displacement and glucose absorption) a much better fit between the diffusion model and the experiment could be achieved (the solid line of figure 7(b)) that confirms most of the experimental spectrum's features. Differences for  $\lambda > 950$  nm can be attributed to larger errors in all experimental absorption and scattering spectra.

### 3.3. The influence of glucose upon phase shift

In a second experiment in a slab geometry ( $L = 20$  mm) the dependence of intensity and phase shift of the transmitted light upon the glucose concentration was investigated. The phantom consisted of an aqueous suspension of the same polystyrene microspheres ( $4 \mu\text{m} < d < 7 \mu\text{m}$ ) as used above, whose absorption had been increased by adding a water-soluble dye (S109564, ICI, Manchester). For the concentrations used (spheres,  $c_s = 5.4\%$  v/v; dye,  $c_d = 0.0185\%$  v/v) and  $\lambda = 804$  nm the resulting optical properties were a modified scattering coefficient  $\mu'_s = 4.8 \text{ mm}^{-1}$  and an absorption coefficient  $\mu_a = 0.016 \text{ mm}^{-1}$ . A high scattering coefficient was chosen to increase the glucose effect. Glucose concentration  $c_g$  was changed between 0 mM and 400 mM by adding an aqueous solution of the same sphere and dye concentration but high glucose concentration. Therefore, the sphere and dye concentration was unchanged during the experiment. The set-up used here to record intensity and phase data consisted of four laser diodes of different wavelengths between 690 nm and 860 nm that were intensity modulated with a frequency  $\nu_M = 200$  MHz in combination with a phase-sensitive PMT detector. Details of this frequency domain system have been given elsewhere (Duncan et al 1993).

In figure 8(a) the measured change in attenuation  $A$ , in units of optical densities OD,  $A = \log_{10}[I(c_g = 0 \text{ mM})/I(c_g)]$ , where  $I(c_g)$  is the measured intensity at concentration  $c_g$ , and the phase shift  $\Delta\Phi = \Phi(c_g) - \Phi(c_g = 0 \text{ mM})$  are plotted versus  $c_g$  ( $\lambda = 804$  nm). Both show an approximately linear dependence. Using the values for  $\mu'_s$ ,  $\mu_a$ ,  $n_m$  and  $n_r$  as well as their changes ( $\delta_g\mu'_s = -0.015\%$  mM $^{-1}$  for 804 nm,  $\Delta_g n_m = 2.5 \times 10^5$  mM $^{-1}$ ), the expected changes of attenuation and phase could be calculated from diffusion theory (3), (5) and the relationship  $\Phi = -2\pi\nu_M t$  (the solid lines in figure 8(a)). Again, the predictions of the diffusion theory are in good agreement with the experimental data.

### 3.4. Separation of absorption and scattering changes

In the last few years it has been shown that the optical properties ( $\mu'_s$ ,  $\mu_a$  and  $n_m$ ) can be determined from measurements of intensity, phase and modulation of an intensity-modulated

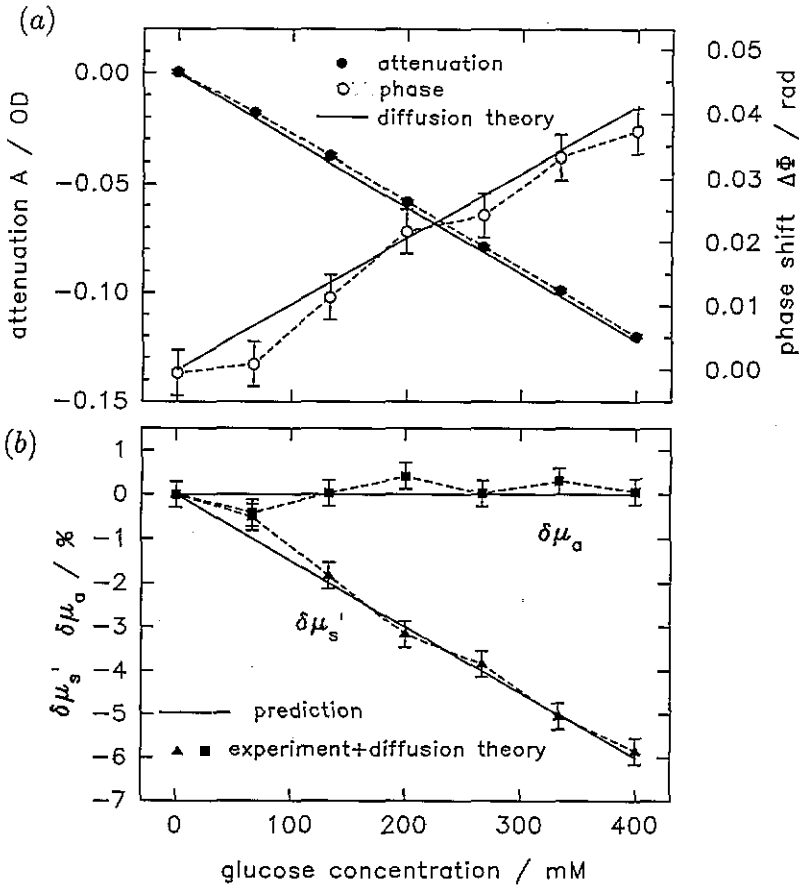


Figure 8. (a) The change in attenuation and phase of transmitted light through a cuvette of 20 mm pathlength versus glucose concentration  $c_g$  for  $\lambda = 804$  nm. The optical properties of the phantom were  $\mu'_s = 4.8 \text{ mm}^{-1}$  and  $\mu_a = 0.016 \text{ mm}^{-1}$  for zero glucose concentration. The experimental data can be compared with predictions based upon Mie and diffusion theory. (b) The separation of fractional changes of scattering and absorption coefficient  $\delta \mu'_s$  (triangles) and  $\delta \mu_a$  (squares) calculated from the experimental data shown in (a) using diffusion theory and the known starting values of  $\mu'_s$  and  $\mu_a$  for  $c_g = 0$ . The expected changes are shown in solid lines: no change for the absorption and a linearly decreasing scattering coefficient.

light source (Patterson *et al* 1991, Tromberg *et al* 1993, Madsen *et al* 1994, Pogue *et al* 1994, Fantini *et al* 1994). Most of these studies use the phase and modulation and their dependence on the modulation frequency for separation and absolute determination of  $\mu'_s$  and  $\mu_a$ . In contrast to phase and modulation, the absolute magnitude of the reflectance is the most difficult to measure and is therefore discarded. Here it is demonstrated that from experimental changes of attenuation ( $\Delta A$ ) and phase ( $\Delta \Phi$ ), changes of scattering and absorption coefficient ( $\delta \mu'_s$ ,  $\delta \mu_a$ ) can be inferred. Preconditions for the separation of  $\delta \mu'_s$  and  $\delta \mu_a$  are that (i) the starting values  $\mu'_s$  and  $\mu_a$  are known and (ii) changes of the refractive index can be either neglected or included. An approximation is made whereby small changes in attenuation and phase can be written as simple linear relations of the fractional changes  $\delta \mu'_s$  and  $\delta \mu_a$ :  $\Delta A = A_s \delta \mu'_s + A_a \delta \mu_a$  and  $\Delta \Phi = \Phi_s \delta \mu'_s + \Phi_a \delta \mu_a$ . This holds in good approximation for the small changes of absorption and scattering considered

here. Therefore,  $\delta\mu'_s$  and  $\delta\mu_a$  can be expressed by

$$\begin{aligned}\delta\mu'_s &= (\Phi_s\Delta A - A_s\Delta\Phi)/(\Phi_s A_a - \Phi_a A_s) \\ \delta\mu_a &= -(\Phi_a\Delta A - A_a\Delta\Phi)/(\Phi_s A_a - \Phi_a A_s).\end{aligned}\quad (8)$$

The constants  $A_s$ ,  $A_a$ ,  $\Phi_s$  and  $\Phi_a$  have to be determined from diffusion theory for the specified starting values  $\mu'_s$  and  $\mu_a$ .

For the experiment performed, the expected fractional changes  $\delta\mu'_s$  and  $\delta\mu_a$  are plotted as solid lines in figure 8(b). The concentration of the dye was held constant. Because the change of water and glucose absorption due to glucose could be neglected, the overall absorption coefficient was constant:  $\delta\mu_a = 0$ . A fractional change of the modified scattering coefficient of  $\delta_g\mu'_s = -1.50\%/100$  mM was derived from Mie theory for the wavelength used. To perform the separation of  $\delta\mu_a$  and  $\delta\mu'_s$  according to (8), for the known starting values  $\mu'_s = 4.8(\pm 0.2)$  mm<sup>-1</sup> and  $\mu_a = 0.0160(\pm 0.003)$  mm<sup>-1</sup>, the changes of attenuation ( $A_s$  and  $A_a$ ) and phase ( $\Phi_s$  and  $\Phi_a$ ) per per cent change of  $\mu'_s$  and  $\mu_a$ , respectively, have been calculated for a slab of 20 mm pathlength from (3) and (5). The refractive index of the medium was taken to be  $n_m = 1.328$  for zero glucose concentration. The Mie prediction of the expected change  $\delta_g\mu'_s = -1.50\%/100$  mM is based upon a change  $\Delta n_m = 0.0025/100$  mM, i.e. a change of the refractive index of  $\Delta n_m = -0.0016$  corresponds to  $\delta_g\mu'_s = 1\%$ . This was incorporated into the calculation of  $\Phi_s$ . Without including this change  $\Delta n_m$ , a slightly different separation of  $\delta\mu'_s$  and  $\delta\mu_a$  would have resulted. For changes of 1% of  $\delta\mu'_s$  and  $\delta\mu_a$ , the following values were calculated: ( $A_s = 0.0208$  OD,  $\Phi_s = -0.00641$  rad) and ( $A_a = 0.01734$  OD,  $\Phi_a = 0.00455$  rad), respectively. Applying these values in (8), the separation of  $\delta\mu'_s$  and  $\delta\mu_a$  shown in figure 8(b) (triangles and squares, respectively) was calculated. Both  $\delta\mu'_s$  and  $\delta\mu_a$  are in good agreement with the expected changes. This confirms both the Mie predictions and the method of  $\delta\mu'_s$ - $\delta\mu_a$  separation.

## 4. Discussion

### 4.1. The effect of glucose on basic optical properties

The magnitude of the effect of dissolved glucose upon optical properties in an aqueous suspension of scattering particles has been described. It has been seen to have four different effects: two upon the absorption coefficient via intrinsic glucose absorption and water displacement and two via refractive index by modifying both the velocity of light and the scattering coefficient. These effects modify the light intensity, modulation depth and phase shift seen in multiple-scattering media that mimic scattering in tissue. These modifications can be described by diffusion theory.

### 4.2. The dependence of the glucose effect upon the absolute absorption coefficient

In figure 7 it has already been shown that the glucose-induced change of the transmittance is reflected in the absolute absorption spectrum of the highly scattering phantom. This needs further examination. In tissue the modified scattering coefficient is fairly wavelength independent (van der Zee et al 1993) while the absorption spectrum is dominated by specific bands of tissue chromophores such as those of haemoglobin or water. In figure 7 the wavelength dependence of  $\mu'_s$  and its change  $\delta_g\mu'_s$  for the polystyrene particles used make it difficult to evaluate the exact influence of  $\mu_a$  on the glucose effect. To clarify this the

$\mu_a$ -dependent fractional change of the transmitted intensity  $\delta T$  has been calculated for a slab of 20 mm pathlength,  $\mu'_s = 1 \text{ mm}^{-1}$  and  $\delta\mu'_s = -1\%$  (figure 9). The advantage of a high background absorption coefficient to produce a high  $\delta T$  can clearly be seen. High absorption strongly reduces the absolute intensity of the detected light. Nevertheless, calculations show that even after reducing the source-detector distance to compensate for this decrease in intensity, the effect is higher for high  $\mu_a$ . Therefore it might be beneficial to choose a wavelength coinciding with a strong absorption band of the tissue, e.g. the bands of water near 975 nm or 1190 nm. Also shown in figure 9 is the change of mean time of flight  $\Delta\langle t \rangle$ , which demonstrates that, in contrast to  $\delta T$ , a low absorption coefficient is advantageous for a high glucose effect.

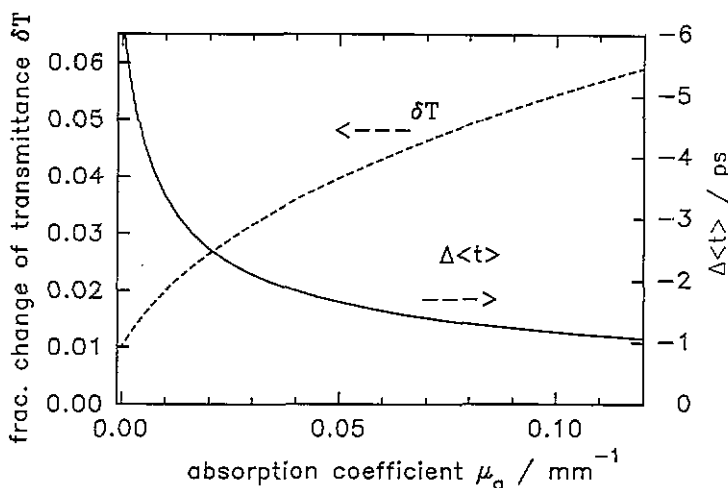


**Figure 9.** The fractional change of transmitted intensity  $\delta T$  and change of mean time of flight  $\Delta\langle t \rangle$  versus absorption coefficient  $\mu_a$ , calculated for a slab of 20 mm pathlength,  $\mu'_s = 1 \text{ mm}^{-1}$ ,  $\delta\mu'_s = -1\%$  and  $n_m = 1.33$ . A matched boundary condition was assumed.

The influence of  $\mu_a$  on the magnitude of the effect may explain why spectroscopic methods have been suggested for *in vivo* monitoring of blood glucose concentration even when the intrinsic glucose absorption itself is negligible.

Perhaps the most surprising result is that intrinsic glucose absorption can be seen in the spectra of these tissue phantoms (figure 7). It appears as a small feature at wavelengths near to 910 nm. Unfortunately the likelihood of seeing this feature in tissue is very small because the conditions in this phantom are somewhat beneficial compared to tissue. Background absorption is very low and glucose concentration very high.

#### 4.3. The influence of refractive index upon the glucose effect and possible interference

The changes of the scattering properties with glucose concentration discussed above are small. However, one distinct possibility is that these changes may be greater in tissue than in the polystyrene particle suspension.

For biological tissue it is hard to predict or estimate  $\delta\mu'_s$ . Tissue scattering is caused by a variety of substances and organelles (membranes, mitochondria, nucleus etc) and fluids that all have different refractive indices varying between values near to that of water

(intracellular and interstitial fluid, blood plasma) to that of protein ( $n \approx 1.5$ ) (Ross 1967). These different refractive indices have to be taken into account. Furthermore, as the sizes of the scattering cell compartments vary between a few tens of a micrometre and a few micrometres, the scattering can only approximately be described by a scattering theory (Mie or Rayleigh theory). Assuming that glucose induces only a change in the refractive index of the medium and that the suspended particle (organelle etc) itself is unaffected, the fractional change  $\delta_g \mu'_s / \text{mM}$  glucose has been calculated from Mie theory for a spherical particle of diameter  $d = 1 \mu\text{m}$  and  $\lambda = 700 \text{ nm}$  as a function of the refractive index  $n_s$  of the sphere (figure 10). A constant refractive index of the medium  $n_m$  of either 1.33 or 1.36 was assumed. The magnitude of  $\delta_g \mu'_s$  shows a large increase as  $n_s$  decreases to values close to that of the medium. This dependence of  $\delta_g \mu'_s$  on  $n_s$  is approximately the same as expected for a pure Rayleigh scatterer whose scattering intensity is proportional to  $I \sim [(n_s/n_m)^2 - 1]/[(n_s/n_m)^2 + 2]^2$  (the dashed line in figure 10). Experimentally it has been confirmed that for the lower refractive index of Intralipid (a soybean oil suspension,  $n_s \approx 1.465$ )  $\delta_g \mu'_s$  is roughly a factor of two larger than for polystyrene ( $n_s = 1.584$ ,  $\delta_g \mu'_s = -0.02\% \text{ mM}^{-1}$ ). For even smaller values of  $n_s$  the expected change is larger.

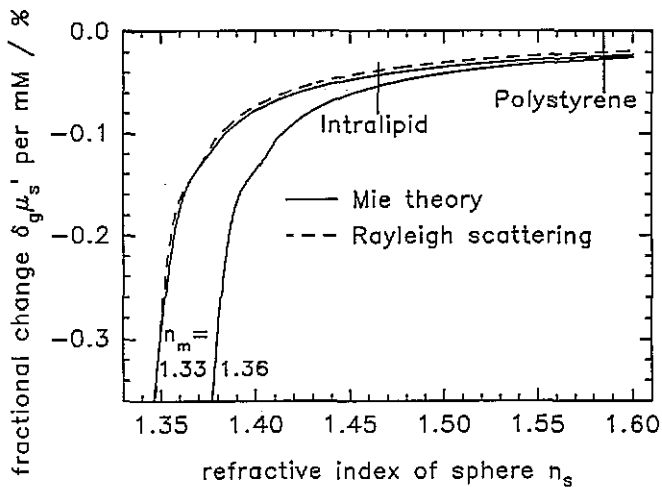


Figure 10. The fractional change  $\delta_g \mu'_s / \text{mM}$  change of glucose concentration as function of the refractive index of the sphere  $n_s$  surrounded by a medium of  $n_m = 1.33$  and  $1.36$  calculated from Mie theory. A wavelength of  $\lambda = 700 \text{ nm}$  and a diameter  $d = 1 \mu\text{m}$  was assumed. For  $n_s = 1.33$ ,  $\delta_g \mu'_s$  can be compared with predictions for a pure Rayleigh scatterer.

Different types of tissue have mean refractive indices ranging from about 1.40 for muscle to 1.46 for adipose (fat) tissue (Bolin *et al* 1989). Assuming that the extracellular fluid of all tissues has about the same refractive index ( $n_m \approx 1.34\text{--}1.35$ ), figure 10 predicts changes of about  $-0.10\%$  and  $-0.05\% \text{ mM}^{-1}$ , respectively, for these tissues. To optimize the glucose effect *in vivo*, it may well be advantageous to choose a position on the body to maximize the signal from tissue with scattering centres of low relative refractive index.

Besides that, the distribution of glucose in tissue and its effect on other physiological parameters is a complex issue. The method suggested here is sensitive to average changes of the refractive index and scattering coefficient of tissue. Therefore, it is not likely to measure the glucose concentration of blood but an average concentration in tissue. This

concentration depends on both the diffusion of the glucose in the tissue and its active uptake into cells, i.e. it may result in differences of the absolute values as well as a certain time delay compared with blood glucose concentration.

Further physiological questions also have to be clarified. The estimation given above assumes that glucose only affects the refractive index of the medium (i.e. the extracellular body fluids) while the particle (cell, organelle etc) is unaffected. In diabetic patients the glucose uptake of the cells is reduced or inhibited. Nevertheless, the glucose concentration certainly induces changes of the concentration of solutes in both the extracellular and intracellular fluids and the metabolism. In diabetic patients there is a glucose correlated increase of the osmolarity of the body fluids and a change of their composition (e.g. electrolytes, urea and ketone bodies) (Wilson *et al* 1991). Any accurate estimation of changes of the refractive index has to sum up all of these different contributions. The overall body fluid balance as well as the renal function is influenced by both the glucose concentration and the osmolarity of body fluids and may induce a further change of the refractive index.

The other parameter most likely to affect the scattering coefficient is the temperature of the tissue. For Intralipid in water, a change of the scattering coefficient  $\delta\mu_s = -0.4\% \text{ } ^\circ\text{C}$  was measured for  $\lambda = 700 \text{ nm}$ . This is in agreement with Mie calculations taking into account temperature changes of the refractive index of water (Weast 1974) and of oils and fats ( $\Delta n \cong -4 \times 10^{-4} \text{ } ^\circ\text{C}$ ; Glasser 1950). This points to the importance of monitoring tissue temperature and the need for additional experiments to measure the scattering in tissue as a function of temperature.

## 5. Conclusion

The experimental and theoretical investigations above have proven the existence of glucose effects upon scattering media. The most significant of these effects was the modification of the reduced scattering coefficient and even this effect was small. Glucose concentrations an order of magnitude greater than physiological levels were needed to obtain measurable effects in tissue phantoms. It is hoped that the glucose effect in tissue is much greater than in these phantoms. Preliminary results in adult volunteers suggest this may be so (Maier *et al* 1994); otherwise instrumentation with greater sensitivity than the current state of the art will be required.

The general agreement between theory and experiment in phantom studies gives confidence in using the basic data and these methods to predict effects for other wavelengths and measurement regimes and to separate changes in absorption and scattering coefficient. The disadvantage of this method is that *changes* rather than absolute values of scattering and absorption coefficient were calculated. However, compared with an absolute determination of  $\mu'_s$  and  $\mu_a$  based upon phase and modulation depth, the potential advantage of using attenuation and phase changes is a lower noise level. Absolute values of tissue scattering are unlikely to be useful in determining absolute glucose concentrations. This technique is likely to require an *in vivo* calibration using blood samples.

The potential application of these findings for the non-invasive monitoring of glucose concentrations in diabetic patients has been discussed. Future studies with diabetic patients have to prove the magnitude of glucose-correlated changes of optical signals and the feasibility of on-line monitoring.

## Acknowledgments

This work was supported by Boehringer Mannheim GmbH, Germany. The development of the intensity-modulated spectrophotometer was supported by The Wellcome Trust.

## References

- Arnold M A and Small G W 1990 Determination of physiological levels of glucose in an aqueous matrix with digitally filtered Fourier transform near-infrared spectra *Anal. Chem.* **62** 1457-64
- Arridge S, Cope M and Delpy D T 1992 The theoretical basis for the determination of optical pathlengths in tissue: temporal and frequency analysis *Phys. Med. Biol.* **37** 1531-60
- Bohren C F and Huffman D R 1983 *Absorption and Scattering of Light by Small Particles* (New York: Wiley)
- Bolin F P, Preuss L E, Taylor R C and Ferenec R J 1989 Refractive index of some mammalian tissues using a fiber optic cladding method *Appl. Opt.* **23** 2297-303
- Cope M 1991 *The development of a near infrared spectroscopy system and its application for non invasive monitoring of cerebral blood and tissue oxygenation in the newborn infant PhD Thesis* University of London
- DCCT Research Group 1993 The effect of intensive treatment of diabetes on the development and progression of long-term complications in insulin-dependent diabetes mellitus *New Engl. J. Med.* **329** 977-86
- Duncan A, Whitlock T L, Cope M, Delpy D T 1993 A multiwavelength, wideband, intensity modulated optical spectrometer for near infrared spectroscopy and imaging *Proc. SPIE* **1888** 248-57
- Fantini S, Franceschini M A, Fishkin J B, Barbieri B and Gratton E 1994 Quantitative determination of the absorption spectra of chromophores in strongly scattering media: a light-emitting diode based technique *Appl. Opt.* **33** 5204-13
- Farrell T J and Patterson M S 1992 A diffusion theory model of spatially resolved, steady-state diffuse reflectance for the non-invasive determination of tissue optical properties *in vivo Med. Phys.* **19** 879-88
- Firbank M, Hiraoka M, Essenpreis M and Delpy D T 1993 Measurement of the optical properties of the skull in the wavelength range 650-950 nm *Phys. Med. Biol.* **38** 503-10
- Glasser O (ed) 1950 *Medical Physics* (Chicago, IL: Year Book) p 1222
- Hale G M and Querry M R 1973 Optical constants of water in the 200 nm to 200  $\mu\text{m}$  wavelength region *Appl. Opt.* **12** 555-63
- Hecht E 1987 *Optics* (Reading, MA: Addison-Wesley)
- Kajiwara D, Uemura T, Kishikawa H, Nishida K, Hashiguchi Y, Uehara M, Sakakida M, Ilchinose K and Shichiri M 1993 Noninvasive measurement of blood glucose concentration by analysing Fourier transform infra-red absorbance spectra through oral mucosa *Med. Biol. Eng. Comput.* **31** S17-22
- Kaye G W and Laby T H 1986 *Tables of Physical and Chemical Constants* (London: Longman)
- Keijzer M, Star W M and Storch P R M 1988 Optical diffusion in layered media *Appl. Opt.* **27** 1820-4
- Kohl M, Cope M, Essenpreis M and Böcker D 1994 Influence of glucose concentration upon light scattering in tissue-simulating phantoms *Opt. Lett.* **19** 2170-2
- Kong J A 1986 *Theory of Electromagnetic Waves* (New York: Wiley)
- Kou L, Labrie D and Chylek P 1993 Refractive indices of water and ice in the 0.65-2.5  $\mu\text{m}$  spectral range *Appl. Opt.* **32** 3531-40
- Madsen S J, Wyss P, Svaasand L O, Haskell R C, Tadr Y and Tromberg B J 1994 Determination of the optical properties of the human uterus using frequency-domain photon migration and steady-state techniques *Phys. Med. Biol.* **39** 1191-202
- Maier J, Walker S, Fantini S, Franceschini M and Gratton E 1994 Non-invasive glucose determination by measuring variations of the reduced scattering coefficient of tissues in the near-infrared *Opt. Lett.* **19** 2062-4
- Marbach R, Koschinsky Th, Gries F A and Heise H M 1993 Noninvasive blood glucose assay by near-infrared diffuse reflectance spectroscopy of the human inner lip *Appl. Spectrosc.* **47** 875
- Moulton D J 1990 Diffusion modelling of picosecond laser pulse propagation in turbid media *Master Thesis* McMaster University
- Patterson M S, Chance B and Wilson B C 1989 Time resolved reflectance and transmittance for the non-invasive measurement of tissue optical properties *Appl. Opt.* **28** 2331-6
- Patterson M S, Moulton J D, Wilson B C, Berndt K W and Lakowicz J R 1991 Frequency-domain reflectance for the determination of the scattering and absorption properties of tissue *Appl. Opt.* **30** 4474-6
- Pogue B W and Patterson M S 1994 Frequency-domain optical absorption spectroscopy of finite tissue volumes using diffusion theory *Phys. Med. Biol.* **39** 1157-80

- Quan K M, Christison G B, MacKenzie H A and Hodgson P 1993 Glucose determination by a pulsed photoacoustic technique: an experimental study using a gelatin-based tissue phantom *Phys. Med. Biol.* **38** 1911–22
- Ross K F A 1967 *Phase Contrast and Interference Microscopy for Cell Biologists* (London: Arnold)
- Robinson M, Eaton R P, Haaland D M, Koeppe D W, Thomas E V, Stallard B R and Robinson P L 1992 Noninvasive glucose monitoring in diabetic patients: a preliminary evaluation *Clin. Chem.* **38** 1618–22
- Simonsen J H and Böcker D 1994 Process and device for glucose determination in a biological matrix *Patent* WO 94/10901
- Tromberg B J, Svaasand L O, Tsay T-T and Haskell R C 1993 Properties of photon density waves in multiple-scattering media *Appl. Opt.* **32** 607–16
- van der Zee P, Essenpreis M and Delpy D T 1993 Optical properties of brain tissue *Proc. SPIE* **1888** 454–65
- Weast R C (ed) 1974 *Handbook of Chemistry and Physics* (Cleveland, OH: Chemical Rubber Company)
- Wilson G S, Zhang Y, Reach G, Moatti-Sirat D, Poitout V, Thévenot D R, Lemonnier F and Klein J-C 1992 Progress toward the development of an implantable sensor for glucose *Clin. Chem.* **38** 1613–17
- Wilson J D, Braunwald E, Isselbacher K J, Petersdorf R G, Martin J B, Fauci A S and Root R K (ed) 1991 *Harrison's Principles of Internal Medicine* 12th edn (New York: McGraw-Hill)